Inorganic Chemistry

Communication

pubs.acs.org/IC

Self-Assembled Bilayers on Indium–Tin Oxide (SAB-ITO) Electrodes: A Design for Chromophore–Catalyst Photoanodes

Christopher R. K. Glasson,[†,‡] Wenjing Song,[†] Dennis L. Ashford,[†] Aaron Vannucci,[†] Zuofeng Chen,[†] Javier J. Concepcion,[†] Patrick L. Holland,[§] and Thomas J. Meyer*[,†]

[†]Department of Chemistry, University of North Carolina, Chapel Hill, North Carolina 27599-3290, United States

[§]Department of Chemistry, University of Rochester, Rochester, New York 14618, United States

Supporting Information

ABSTRACT: A novel approach for creating assemblies on metal oxide surfaces via the addition of a catalyst overlayer on a chomophore monolayer derivatized surface is described. It is based on the sequential self-assembly of a chromophore, $[Ru(bpy)(4,4'\text{-}(PO_3H_2bpy)_2)]^{2+}$, and oxidation catalyst, $[Ru(bpy)(P_2Mebim_2py)OH_2]^{2+}$, pair, resulting in a spatially separated chromophore–catalyst assembly.

Dye-sensitized photoelectrosynthesis cells (DSPECs) provide a promising approach to solar fuels by water splitting into hydrogen and oxygen (eq 1) or CO_2 reduction to CO, other oxygenates, or hydrocarbons (eq 2).[1−5] One design features a photoanode consisting of a visible-light absorber chemically linked to a water oxidation catalyst on the surface of TiO_2 or another high-band-gap metal oxide semiconductor. Excitation and injection into the semiconductor by the chromophore is followed by intra-assembly electron-transfer activation of the catalyst. The success of these designs relies on efficient light absorption, injection, and electron-transfer activation of the catalyst before back electron transfer between TiO_2 (e^-) and the oxidized catalyst can occur.

$$2H_2O + 4h\nu \rightarrow O_2 + 2H_2 \quad (1)$$

$$2H_2O + CO_2 + 8h\nu \rightarrow 2O_2 + CH_4 \quad (2)$$

Back electron transfer is especially problematic for solar fuel half-reactions given their multiple-electron, multiple-proton demands, e.g., $2H_2O \rightarrow O_2 + 4H^+ + 4e^-$, and the requirement to build up multiple oxidative equivalents to avoid high-energy $1e^-$ intermediates. These design requirements impose significant rate constraints and dynamic control issues on the linkage between the catalyst and chromophore.

A number of approaches are under investigation. They fit generally into two broad categories; covalently linked[5−8] and noncovalently linked assemblies.[9] As an example of the former, the results of a photophysical study on the chromophore–catalyst assembly, $[(dcb)_2Ru(bpy\text{-}Mebim_2py)Ru(bpy)(OH_2)]^{4+}$ $[Ru_a^{II}–Ru_b^{II}OH_2$; dcb = 4,4′-dicarboxylic acid-2,2′-bipyridine, bpy-Mebim$_2$py = 2,2′-(4-methyl-[2,2′:4′,4″-terpyridine]-2-diyl)bis(1-methyl-1*H*-benzo[*d*]imidazole), and bpy = 2,2′-bipyridine], on TiO_2 have appeared.[7] Mallouk and coworkers have demonstrated water splitting with an applied bias at TiO_2 surfaces derivatized with a phosphonate-derivatized $Ru^{II}(bpy)_3$ complex having a pendant malonate group for binding $IrO_2{\cdot}nH_2O$ nanoparticles.[8] A multilayer approach was reported by Spiccia and co-workers in which a surface-bound chromophore on fluorine-doped tin oxide was overlaid with an outer layer containing a manganese–oxo cluster ion exchanged into Nafion.[9]

Here we report a novel approach to surface-bound chromophore–catalyst assemblies. The strategy is based on a self-assembled bilayer (SAB), in which a catalyst monolayer overlays a chromophore monolayer on a tin(IV)-doped In_2O_3 (ITO) electrode. It consists of a noncovalently associated, but spatially overlapping, chromophore $[Ru(bpy)(4,4\text{-}(PO_3H_2bpy)_2)]^{2+}$ (**1**; bpy = 2,2′-bipyridine) and catalyst $[Ru(bpy)(P_2Mebim_2py)OH_2](OTf)_2$ (**2**; P_2Mebim_2py = 2,6-bis[1-(10-diethylphosphonyl)decylbenzimidazol-2-yl]pyridine); note Scheme 1.

Scheme 1

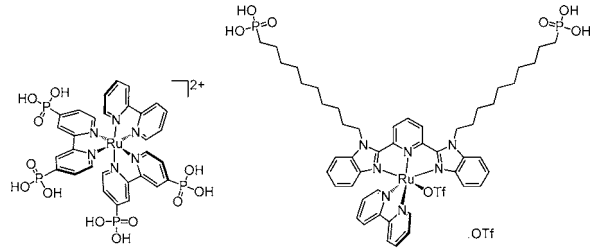

1 **2**

Catalyst **2** has pendant alkyl chains with $(CH_2)_{10}$ spacers (∼15 Å fully extended) and terminal phosphonic acid groups. The latter was designed such that surface attachment of catalyst **2** could be achieved on metal oxide surfaces prederivatized with chromophore **1** (diameter ∼13 Å). We report here the successful application of this strategy and the electrochemical behavior of the resulting SAB.

Components **1**[10] and **2**[7] were prepared by literature procedures. P_2Mebim_2py was prepared by the treatment of 2,6-bis(1*H*-benzo[*d*]imidazol-2-yl)pyridine[11] with NaH in *N*,*N*-dimethylformamide (DMF) and subsequent reaction with diethyl(10-bromodecyl)phosphonate.[12] ^{1}H NMR spectroscopy and high-resolution mass spectrometry (HRMS) confirmed the

Received: March 26, 2012
Published: August 2, 2012

   dx.doi.org/10.1021/ic300636w | *Inorg. Chem.* 2012, 51, 8637−8639

formation of P_2Mebim_2py [see the Supporting Information (SI), section S1]. The catalyst was prepared by the reaction of $[Ru(bpy)(bz)(OTf)](OTf)$[10] (bz = benzene) with P_2Mebim_2py in a refluxing ethanol−water mixture and purified by column chromatography on silica gel. The ^1H NMR spectrum was consistent with the formation of **2**, and its composition was confirmed by HRMS (see the SI, section S1). The phosphonate esters were solvolyzed by TMSBr in DMF.[12]

A series of qualitative loading experiments allowed the SAB surface attachment design principles to be validated (see the SI, section S2) and were used to create surface structures. SAB-ITO electrodes were prepared in a two-step sequence. Fully loaded ITO slides, derviatized with **1**, were prepared by literature methods.[13,14] The surface coverage, Γ in mol/cm^2, was calculated from the areas of cyclic voltammetric (CV) waves (A in cm^2) from the expression $\Gamma = Q/nFA$, with n the electrochemical stoichiometry and F the Faraday constant.[13−15] Calculated surface coverages were typically on the order of $\Gamma \sim 1.1 \times 10^{-10}$ mol/cm^2, in good agreement with the theoretical value of 1.2×10^{-10} mol/cm^2 for a close-packed surface.[13,15]

The second step in the preparation of SAB-ITO electrodes was immersion of chromophore-derivatized ITO slides in $\sim 5 \times 10^{-5}$ M dichloromethane solutions in **2** for 24 h followed by sonication in methanol to remove unbound **2**. Integration of the current−potential waveform for the $Ru^{III/II}$ couple of **2** suggested surface coverages on the order of $\Gamma \sim 6 \times 10^{-11}$ mol/cm^2. Similar surface coverages were observed on ITO electrodes derivatized only by **2**. These values are ∼15% less than the maximum surface coverage of $\Gamma \sim 7.0 \times 10^{-11}$ mol/cm^2 estimated from van der Waals radii for **2** (see the SI, section S3). Loading **2** onto ITO slides from more polar solvents led to a significant decrease in surface coverage. For example, when **2** was loaded onto ITO electrodes from methanol, surface coverages were typically halved, to $\Gamma \sim 3 \times 10^{-11}$ mol/cm^2. Loading **2** from methanol onto ITO derivatized by **1** led to surface coverages comparable to $\Gamma \sim 3 \times 10^{-11}$ mol/cm^2.

Both **2** and a related surface-bound analogue, $[Ru(Mebim_2py)(4,4'\text{-}(CH_2PO_3H_2)_2(bpy))(OH_2)]^{2+}$ (**3**),[16] are well-behaved electrochemically on ITO, as shown by CV measurements. For **1**, $E_{1/2}$ = 1.41 V vs NHE for the $Ru^{III/II}$ couple in 0.1 M HNO_3. For **2** on ITO in 0.1 M HNO_3, $E_{1/2}$ = 0.82 and 1.29 V vs NHE for the $Ru^{III}OH_2^{3+}/Ru^{II}OH_2^{2+}$ and $Ru^{IV}{=}O^{2+}/Ru^{III}OH_2^{3+}$ couples and at $E_{p,a} \sim 1.67$ V for the $Ru^{V}{=}O^{3+}/Ru^{IV}{=}O^{2+}$ couple (Figure 1). The wave for the $Ru^{V}{=}O^{3+}/Ru^{IV}{=}O^{2+}$ couple appears at the onset of a catalytic wave for water oxidation. For **3**, the corresponding waves appear at $E_{1/2}$ = 0.83 and 1.25 V and $E_{p,a} \sim 1.65$ V.

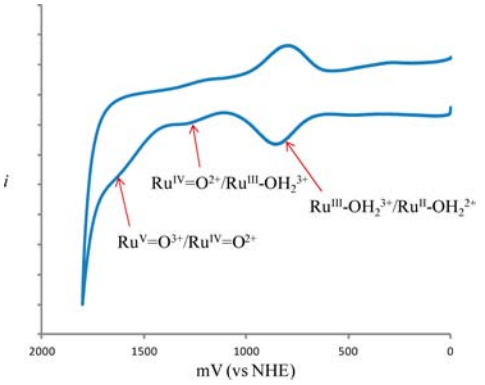

Figure 1. Cyclic voltammogram for an ITO electrode (∼1 cm^2) derivatized with catalyst **2** in 0.1 M HNO_3 (scan rate of 100 mV/s at 22 °C).

As previously reported, slow kinetics are observed for the $1e^-/2H^+$ $Ru^{IV}{=}O^{2+}/Ru^{III}OH_2^{3+}$ couple due to its proton-coupled electron-transfer mechanism.[17,18] Sluggish kinetics lead to smaller than expected peak currents due to the partial oxidation of $Ru^{III}OH_2^{3+}$ on the surface of the electrode on the CV time scale. The expected pH-dependent behavior for catalyst **2**, for both the $Ru^{III/II}$ and $Ru^{IV/III}$ couples, was significantly modified in the SAB bilayer.[17] Between pH 1 and 2, $E_{1/2}$ for the $Ru^{III/II}$ and $Ru^{IV/III}$ couples varied by ∼59 and ∼120 mV/pH units, consistent with $Ru^{III}OH^{2+}/Ru^{II}OH_2^{2+}$ ($E_{1/2} \sim 0.83$ V) and $Ru^{IV}{=}O^{2+}/Ru^{III}OH_2^{2+}$ ($E_{1/2} \sim 1.13$ V) couples, respectively. However, the electrode response was dependent on the number of CV scans because of instability at the catalyst; see below.

In the cyclic voltammogram of the SAB-ITO electrode in Figure 2, the potential for the $Ru^{III}OH_2^{3+}/Ru^{II}OH_2^{2+}$ couple

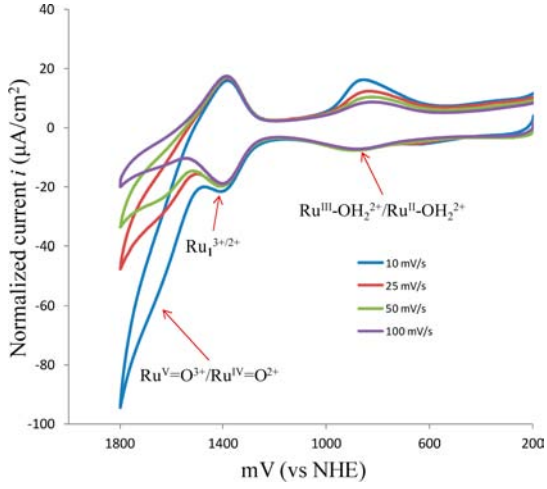

Figure 2. Normalized cyclic voltamograms (i_p/v) for a SAB-ITO electrode with chromophore **1** ($\Gamma \sim 1.1 \times 10^{-10}$ mol/cm^2) and catalyst **2** ($\Gamma \sim 7.0 \times 10^{-11}$ mol/cm^2) in 0.1 M HNO_3 at 22 °C.

increased by ∼50 mV to 0.88 V vs NHE, as a consequence of the chromophore underlayer. The $Ru^{IV}{=}O^{2+}/Ru^{III}OH_2^{3+}$ catalyst couple was masked by the chromophore $Ru^{III/II}$ couple at 1.39 V. The wave for the $Ru^{V}{=}O^{3+}/Ru^{IV}{=}O^{2+}$ couple overlapped with the onset of catalytic water oxidation at ∼1.65 V vs NHE. The scan-rate-dependent behavior for the latter in Figure 2 is revealing. It points to electrocatalysis with relatively slow (tens of seconds time scale) water oxidation catalysis following an oxidative scan into the external $Ru^{V}{=}O^{3+}/Ru^{IV}{=}O^{2+}$ couple. It is also notable that catalysis is initiated at 1.48 V, consistent with electron-transfer mediation; this is based on the potential for the chromophore $Ru^{III/II}$ couple and its nearly diffusion-controlled self-exchange rate (see Figure S2.2 in the SI).[6,19]

Although the CV results provide clear evidence for catalytic water oxidation by the chromophore−catalyst SAB, sustained currents over extended periods required to measure oxygen were not obtainable. Controlled potential electrolysis on *nano*-ITO at 1.8 V (vs NHE) in 0.1 M $HClO_4$ resulted in rapid loss of current to the background and a shift in potential for the catalyst $Ru^{III/II}$ couple to ∼0.75 V (see the SI, section S4).

dx.doi.org/10.1021/ic300636w | *Inorg. Chem.* 2012, 51, 8637−8639

Similar behavior was observed in 0.1 M HNO_3 and in a pH 5 acetate buffer.

A possible deactivation mechanism is suggested by the shift in potential for the catalyst $Ru^{III/II}$ couple and by HRMS data on **2**, which revealed the appearance of a 2+ ion with mass 504.6677 corresponding to the nominally five-coordinate form, $[Ru(bpy)(P_2Mebim_2py)]^{2+}$. The catalyst, as its phosphonate ester, also gave a 2+ ion with mass $[560.7295]^{2+}$ consistent with $[Ru(bpy)(P_2Mebim_2py)]^{2+}$. A related behavior on the surface would explain this result and the negative shift in potential for the $Ru^{III/II}$ couple as arising from the displacement of coordinated H_2O by the anionic phosphonate. Molecular models show that intramolecular coordination of a phosphonate arm such as $-(CH_2)_9PO(OH)O-Ru$ is feasible (see the SI, section S4). Phosphonate coordination in this case may involve oxidation and oxygen release with the subsequent capture of the five-coordinate intermediate by a phosphonate arm. Note that the small quantities of complex available following removal from the surface and the presence of paramagnetic impurities prevent further elucidation of the product by NMR spectroscopy.

The stability of the SAB structure toward loss from the surface at higher pH values was comparable to surface-bound **1**. This was demonstrated by a series of repetitive CV scans with comparisons in integrated peak currents for the $Ru^{III/II}$ waves for SAB-ITO and **1** on ITO in a pH 7.0, 0.1 M phosphate buffer. Following 60 scans from 0.2 to 1.6 V at a scan rate of 100 mV/s, there was a 54% loss in current for the SAB and 46% loss for **1** (see the SI, section S5).

Although there are clearly limitations to this initial approach to SAB structures, our results demonstrate the feasibility of a new design principle for assembling chromophore−catalyst combinations on metal oxide surfaces. It is based on the assembly of an overlayer through sequential addition with overlayer surface binding. This approach avoids the often tedious synthesis of a covalently linked chromophore−quencher assembly. It adds synthetic flexibility in assembling the catalyst overlayer, which, in a properly designed system, may allow control over deleterious back electron transfer and enhance surface stability.

■ ASSOCIATED CONTENT

Ⓢ Supporting Information

Synthetic procedures and characterization of water oxidation catalyst **2** as well as related electrochemical data and modeling procedures. This material is available free of charge via the Internet at http://pubs.acs.org.

■ AUTHOR INFORMATION

Corresponding Author

*E-mail: tjmeyer@unc.edu.

Present Address

‡School of Pharmacy and Molecular Sciences, James Cook University, Townsville, Queensland 4814, Australia.

Notes

The authors declare no competing financial interest.

■ ACKNOWLEDGMENTS

This work was funded by the UNC Energy Frontier Research Center (EFRC), "Center for Solar Fuels", an EFRC funded by the U.S. Department of Energy, Office of Science, Office of Basic Energy Sciences, under Award DE-SC0001011, supporting synthetic and electrochemical analysis (J.J.C.). Funding for materials preparation and electrochemistry by C.R.K.G., Z.C., and A.V. was provided by the Army Research Office through Grant W911NF-09-1-0426. Partial funding for electrochemical analysis by W.S. and C.R.K.G. was provided by the CCHF, an EFRC funded by the U.S. Department of Energy, Office of Science, Office of Basic Energy Sciences, under Award DE-SC0001298 at the University of Virginia, which is also gratefully acknowledged. We also acknowledge support for A.V. and the purchase of instrumentation by UNC EFRC (Center for Solar Fuels), an EFRC funded by the U.S. Department of Energy, Office of Science, Office of Basic Energy Sciences, under Award DE-SC0001011.

■ REFERENCES

(1) Treadway, J. A.; Moss, J. A.; Meyer, T. J. *Inorg. Chem.* **1999**, *38*, 4386−4387.

(2) Song, W.; Chen, Z.; Brennaman, M. K.; Concepcion, J. J.; Patrocinio, A. O. T.; Iha, N. Y. M.; Meyer, T. J. *Pure Appl. Chem.* **2011**, *83*, 749−768.

(3) (a) Alstrum-Acevedo, J. H.; Brennaman, M. K.; Meyer, T. J. *Inorg. Chem.* **2005**, *44*, 6802−6827. (b) Huynh, M. H. V.; Dattelbaum, D. M.; Meyer, T. J. *Coord. Chem. Rev.* **2005**, *249*, 457−483. (c) Concepcion, J. J.; Jurss, J. W.; Brennaman, M. K.; Hoertz, P. G.; Patrocinio, A. O. T.; Iha, N. Y. M.; Templeton, J. L.; Meyer, T. J. *Acc. Chem. Res.* **2009**, *42*, 1954−1965.

(4) (a) Wasielewski, M. R. *Acc. Chem. Res.* **2009**, *42*, 1910−1921. (b) Wasielewski, M. R. *Chem. Rev.* **1992**, *92*, 435−461.

(5) Youngblood, W. J.; Lee, S.-H. A.; Maeda, K.; Mallouk, T. E. *Acc. Chem. Res.* **2009**, *42*, 1966−1973.

(6) Concepcion, J. J.; Jurss, J. W.; Hoertz, P. G.; Meyer, T. J. *Angew. Chem., Int. Ed.* **2009**, *48*, 9473−9476.

(7) Song, W.; Glasson, C. R. K.; Luo, H.; Hanson, K.; Brennaman, M. K.; Concepcion, J. J.; Meyer, T. J. *J. Phys. Chem. Lett.* **2011**, 1808−1813.

(8) Youngblood, W. J.; Lee, S.-H. A.; Kobayashi, Y.; Hernandez-Pagan, E. A.; Hoertz, P. G.; Moore, T. A.; Moore, A. L.; Gust, D.; Mallouk, T. E. *J. Am. Chem. Soc.* **2009**, *131*, 926−927.

(9) Brimblecombe, R.; Koo, A.; Dismukes, G. C.; Swiegers, G. F.; Spiccia, L. *J. Am. Chem. Soc.* **2010**, *132*, 2892−2894.

(10) Gillaizeau-Gauthier, I.; Odobel, F.; Alebbi, M.; Argazzi, R.; Costa, E.; Bignozzi, C. A.; Qu, P.; Meyer, G. J. *Inorg. Chem.* **2001**, *40*, 6073−6079.

(11) Rowan, S. J.; Beck, J. B. *Faraday Discuss.* **2005**, *128*, 43−53.

(12) Terada, K.; Kobayashi, K.; Haga, M. *Dalton Trans.* **2008**, 4846−4854.

(13) Jurss, J. W.; Concepcion, J. J.; Norris, M. R.; Templeton, J. L.; Meyer, T. J. *Inorg. Chem.* **2010**, *49*, 3980−3982.

(14) Gagliardi, C. J.; Jurss, J. W.; Thorp, H. H.; Meyer, T. J. *Inorg. Chem.* **2011**, *50*, 2076−2078.

(15) Meyer, T. J.; Meyer, G. J.; Pfennig, B. W.; Schoonover, J. R.; Timpson, C. J.; Wall, J. F.; Kobusch, C.; Chen, X.; Peek, B. M.; Wall, C. G.; Ou, W.; Erickson, B. W.; Bignozzi, C. A. *Inorg. Chem.* **1994**, *33*, 3952−3964.

(16) Chen, Z.; Concepcion, J. J.; Jurss, J. W.; Meyer, T. J. *J. Am. Chem. Soc.* **2009**, *131*, 15580−15581.

(17) Trammell, S. A.; Wimbish, J. C.; Odobel, F.; Gallagher, L. A.; Narula, P. M.; Meyer, T. J. *J. Am. Chem. Soc.* **1998**, *120*, 13248−13249.

(18) Chen, Z.; Vannucci, A. K.; Concepcion, J. J.; Jurss, J. W.; Meyer, T. J. *Proc. Natl. Acad. Sci. U.S.A.* **2011**, *108*, E1461−E1469.

(19) Concepcion, J. J.; Jurss, J. W.; Templeton, J. L.; Meyer, T. J. *Proc. Natl. Acad. Sci. U.S.A.* **2008**, *105*, 17632−17635.